Journal of Colloid and Interface Science 640 (2023) 1080–1088

Contents lists available at ScienceDirect

Journal of Colloid and Interface Science

journal homepage: www.elsevier.com/locate/jcis

Sustainable regeneration of high-performance $LiCoO_2$ from completely failed lithium-ion batteries

Lingyu Kong [a,b], Zhuo Li [a], Wenhui Zhu [c], Chirag R. Ratwani [b], Niranjala Fernando [b], Shadeepa Karunarathne [b], Amr.M. Abdelkader [b,***], Ali Reza Kamali [c,*], Zhongning Shi [d,**]

[a] Key Laboratory for Ecological Metallurgy of Multimetallic Mineral (Ministry of Education), Northeastern University, Shenyang 110819, China
[b] Department of Design and Engineering, Bournemouth University, Talbot Campus, Poole BH12 5BB, United Kingdom
[c] Energy and Environmental Materials Research Centre (E^2MC), School of Metallurgy, Northeastern University, Shenyang 110819, China
[d] State Key Laboratory of Rolling and Automation, Northeastern University, Shenyang 110819, China

GRAPHICAL ABSTRACT

ARTICLE INFO

Article history:
Received 21 December 2022
Revised 28 February 2023
Accepted 2 March 2023
Available online 7 March 2023

Keywords:
Spent lithium-ion batteries
Batteries recycling
Completely failed cathode material
Environmental and economic assessment
Circular economy

ABSTRACT

Utilising the solid-state synthesis method is an easy and effective way to recycle spent lithium-ion batteries. However, verifying its direct repair effects on completely exhausting cathode materials is necessary. In this work, the optimal conditions for direct repair of completely failed cathode materials by solid-state synthesis are explored. The discharge capacity of spent $LiCoO_2$ cathode material is recovered from 21.7 mAh g^{-1} to 138.9 mAh g^{-1} under the optimal regeneration conditions of 850 °C and n(Li)/n(Co) ratio of 1:1. The regenerated materials show excellent electrochemical performance, even greater than the commercial $LiCoO_2$. In addition, based on the whole closed-loop recycling process, the economic and environmental effects of various recycling techniques and raw materials used in the battery production process are assessed, confirming the superior economic and environmental feasibility of direct regeneration method.

1. Introduction

As an efficient energy storage technology, lithium-ion batteries (LIBs) are widely used in portable electronic devices and electric vehicles due to their outstanding electrochemical performances [1–3]. However, due to the limited lifespan and less than 5% recy-

* Corresponding author.
* Corresponding author.
* Corresponding author.
E-mail addresses: aabdelkader@bournemouth.ac.uk (A.M. Abdelkader), ali@mail.neu.edu.cn (A.R. Kamali), znshi@mail.neu.edu.cn (Z. Shi).

https://doi.org/10.1016/j.jcis.2023.03.021
0021-9797/

cling rate, huge amounts of spent LIBs have been accumulated, causing serious side effects such as resource scarcity, environmental pollution, safety problems, and increased cost [4,5]. With the increasing demand for electric vehicles, this problem is expected to magnify in the next few years. Spent LIBs, known as artificial minerals, can serve as a secondary source of strategic metals such as lithium and cobalt [6–8]. Meanwhile, carcinogenic heavy metals and toxic electrolytes exposed to the environment through spent LIBs may cause serious issues to human health and the environment [9]. Therefore, the recycling of spent LIBs is indispensable for realising the great economic value and environmental protection.

The primary recycling methods can be divided into pyrometallurgy, hydrometallurgy, and direct regeneration [10–12]. High-temperature smelting methods, such as carbothermic and aluminothermic reduction, are among typical pyrometallurgical methods used for recycling of spent batteries, by which valuable metals available in cathode materials can be converted into metal oxides or pure metals [13,14]. Although pyrometallurgy is simple, low recycling efficiency, high energy consumption and secondary pollution caused by these methods are still unavoidable [15,16]. A hydrometallurgical process mainly enriches valuable metals in solution by acid or alkali leaching for subsequent separation and recovery [17–19]. The hydrometallurgical process has the advantages of low energy consumption, high recovery rate and high purity [20,21]. However, complex operation steps, excessive use of corrosive reagents and secondary pollution still need to be dealt with [22,23].

The direct regeneration method is considered the most promising recycling method, which can obtain cathode materials with excellent electrochemical performance and alleviate environmental pollution [24]. Direct regeneration is defined as a process of collecting electrode materials from spent LIBs and reusing them in remanufactured LIBs [25]. The key point here is to heal the structural and compositional defects of spent cathode materials by relithiation and annealing to maximise the retention of the high-added-value of cathode materials [26–28]. Molten salts can provide effective environments for reorganizing of minerals for LIB applications [29]. Yang et al. [30] explored the molten salt treatment of LiOH-KOH-Li_2CO_3 to restore the electrochemical performance of $LiCoO_2$ (LCO). The molten salt mixture (LiOH-KOH-Li_2CO_3) can eliminate impurities [31], supply Li^+ and repair the structure of the material through a "dissolution-recrystallisation" mechanism. Jing et al. [32] proposed a one-step hydrothermal method to regenerate spent $LiFePO_4$ using $Li_2SO_4{\cdot}H_2O$ as the Li^+ source and $N_2H_4{\cdot}H_2O$ as the reductant. The regenerated $LiFePO_4$ displayed an excellent discharge capacity of 146 mAh g^{-1} at 0.2 C. Furthermore, Zhang et al. [33] used an electrochemical relithiation method to directly repair LCO cathode materials, where the spent Li_xCoO_2 was used as the working electrode for Li^+ insertion using Li_2SO_4, followed by annealing at 700 °C. The charge capacity of such regenerated LCO materials was close to that of commercial LCO. Despite encouraging results, these methods invisibly complicate the recycling process, increase the recycling cost, and generate secondary pollution. Wu et al. [34] and Gao et al. [35] tried to develop a more eco-friendly regenerating method by upcycling LCO through Na-doping and Al_2O_3-caoting. However, as with other works in the literature, the materials used in Wu and Gao's research retain a certain capacity, often 100 mAh g^{-1} (around 70% capacity loss) [13,36,37]. To the best of our knowledge, there are no studies on the direct regeneration of completely depleted LIBs.

In this work, the effectiveness of the solid-state synthesis method for direct repair of completely depleted LIBs is explored, and reasons for the complete failure of the electrochemical performance of the spent LCO are verified. In addition, the effects of different calcination temperatures and n(Li)/n(Co) ratio on structural repair are investigated. Furthermore, the economic and environmental impacts of different recycling methods, the entire closed-loop recycling process and the raw materials used in the battery production process are assessed and compared.

2. Experimental section

2.1. Regeneration of spent cathode materials

The regeneration procedure used in this study is shown in Fig. 1. Spent LIBs were fully discharged in saturated NaCl solution for 24 h to avoid short-circuiting and self-ignition, followed by drying in a vacuum drying oven at 70 °C for 8 h. Then, the spent batteries were manually disassembled and separated in a fume cupboard. Next, the cathodes were calcined in a muffle furnace under air atmosphere at 600 °C for 2 h to remove the polyvinylidene fluoride (PVDF) binder and the conductive agent. The obtained spent LCO powder was denoted as SLCO.

The SLCO material was regenerated by the solid-state synthesis in air at different temperatures of 750, 850 and 950 °C, denoted as RLCO750, RLCO850 and RLCO950, respectively. To investigate the effects of the n(Li)/n(Co) ratio on the SLCO regeneration, stoichiometric amounts of Li_2CO_3 were added to achieve the n(Li)/n(Co) ratios of 1:1, 1.03:1, 1.05:1 and 1.1:1, defined as RLCO100, RLCO103, RLCO105 and RLCO110, respectively. Commercial LCO is denoted as CLCO.

2.2. Characterisations

The concentrations of various metal ions in the solutions were determined by inductively coupled plasma optical emission spectroscopy (ICP-OES, Optima 8300DV, PerkinElmer, USA). The crystal structure of the cathode materials was characterised by X-ray diffraction (XRD, D8 Bruker) with Cu K_α radiation (λ = 1.5406 Å). Rietveld refinement was employed using Fullprof software to obtain lattice parameters of different LCO materials. The morphologies of the cathode materials were measured by scanning electron microscopy (SEM, Ultra Plus, Zeiss, Germany).

2.3. Electrochemical performance characterisation

The electrochemical performances of samples were evaluated using half-cells (CR2032) with Li sheet as the anode. A solution of 1 M $LiPF_6$ in ethylene carbonate/ethyl methyl carbonate (EC/EMC, 1:1 in volume) was used as the electrolyte. The slurry was prepared in NMP using 80 wt% LCO as the active material, 10 wt% conductive acetylene black and 10 wt% PVDF binder, and the slurry was coated on Al foil used as the current collector. The electrode was vacuum dried at 80 °C for 12 h. Galvanostatic charge–discharge and rate performance measurements were carried out from 3.0 to 4.3 V (vs Li^+/Li) using a battery testing system (Shenzhen, Neware instrument Co. Ltd., China). In order to activate the batteries, all batteries were charged and discharged for one cycle at 0.1C before testing. Cycle voltammograms (0.2 mV s^{-1}, voltage range 3.0–4.3 V) and electrochemical impedance spectroscopy (EIS, 0.1 MHz to 0.01 Hz) were performed using an electrochemical workstation (CHI660D).

3. Results and discussion

3.1. Failure analysis and characterisations

It is known that the loss of Li in the cathode material of LIBs during long-term cycling leads to the failure of the layered LCO

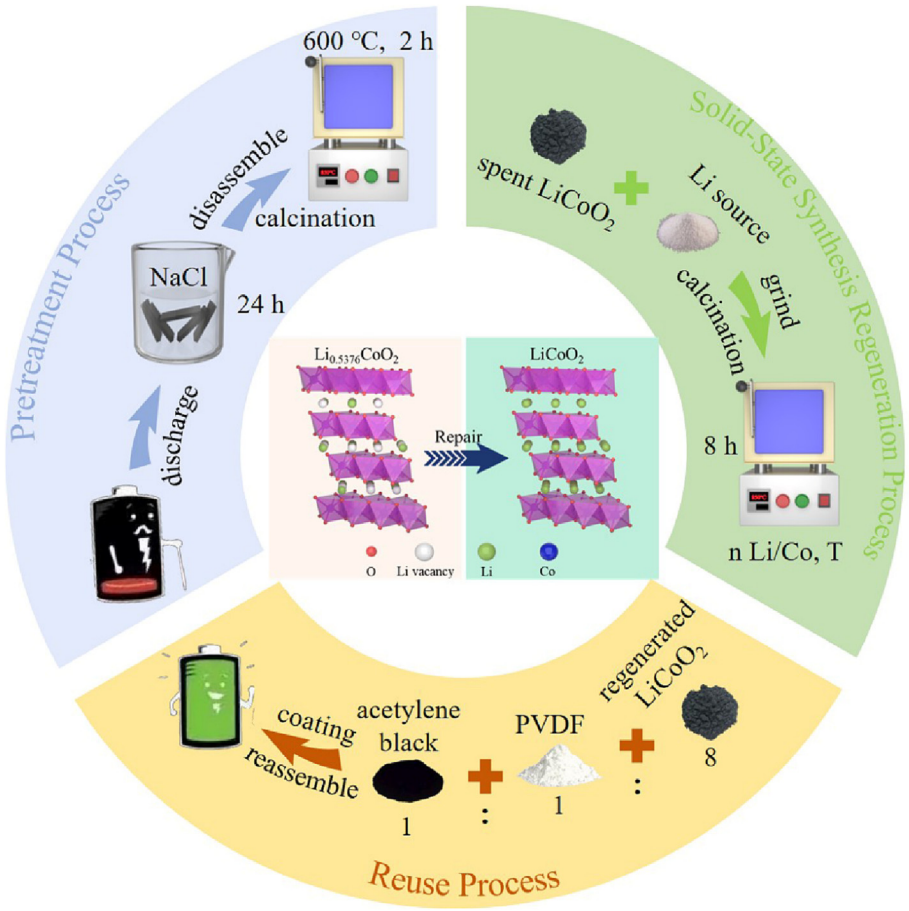

Fig. 1. Illustration of the recycling and regeneration procedure.

structure. The ICP-OES results of spent and regenerated LCO cathode materials are shown in Table S1. Through elemental analysis of the spent cathode material, the residual Li in spent LCO was only 53.76% of its initial content, confirming the lithium loss from the cathode during long-term cycling. The Li loss produces a large number of Li vacancies (Fig. 1), causing significant changes in the LCO crystal structure. The Li depletion also produces surface impurity phases such as spinel and rock salt. The rejuvenation of the composition after regeneration process indicates that the layered structure has been well repaired. The XRD patterns of different samples are shown in Fig. 2. The crystal structures of spent, regenerated, and commercial LCO materials all belong to the hexagonal α-$NaFeO_2$ layered structure with $R\bar{3}m$ space group. It is noticeable that the (003) peak of SLCO shifted to a lower angle (Fig. 2 (b)), corresponding to the increase in the *c* lattice distance due to the electrostatic repulsion between the oxygen layers in the Li deficiency state (Shi et al., 2018b). Moreover, the existence of the Co_3O_4 peaks in the SLCO material indicates an irreversible conversion reaction in the repeated (de)intercalation process (Fig. 2 (c)). After regeneration by solid-state synthesis at 750 °C, the peaks of the Co_3O_4 impurity phase can still be detected, indicating insufficient regeneration reaction. By increasing the temperature to 850 and 950 °C, the Co_3O_4 peak disappears, and no impurity phases are generated. In addition, the clear split peak couples of (006)/(102) and (108)/(110) of regenerated materials indicate ordered layered structures (Fig. 2 (d)). It can be seen from Fig. 2 (e) that increasing the ratio of n(Li)/n(Co) did not lead to the formation of impurity phases, and the regenerated LCO exhibits a well-defined layered structure. The XRD patterns were further analysed by Rietveld refinement and the results are displayed in Fig. S1 and Table S2. Except for SLCO and RLCO750, the *c/a* values of other materials are all over 4.99, indicating a good layered structure. Therefore, based on the above analysis, it can be concluded that the failure and regeneration of LCO may occur based on the following reactions:

$$Li_{1-x}CoO_2 \rightarrow \frac{x}{3}Co_3O_4 + (1-x)LiCoO_2 + \frac{x}{3}O_2 \quad (1)$$

$$2Co_3O_4 + 3Li_2CO_3 + \frac{1}{2}O_2 \rightarrow +6LiCoO_2 + 3CO_2 \quad (2)$$

The SEM images of SLCO (Fig. 3 (a) and (b)) reveal inhomogeneous particle size distribution, with noticeable agglomeration due to the presence of residual PVDF. This inhomogeneity could also result from the ejected impurity phases, such as Co_3O_4. The particles' surfaces are rough with obvious cracks, which are attributed to the inhomogeneous volume changes and internal mechanical stresses introduced on particles due to the repeated insertion and extraction of Li^+. The Li depletion from the LCO phase and the significant structural damage is also accountable for the crack and other defects formations. These defects on the particles' surfaces expand the contact area between the electrolyte and LCO, resulting in more side reactions. In contrast, the regenerated LCO particles have smaller particle size and more uniform distribution. The particle surface is smooth and the layered structure is clearly visible, consistent with the fresh CLCO (Figs. 3 (c)–(f) and S2). Fig. S3 and S4 show the effects of different regeneration temperatures and n(Li)/n(Co) ratios on the morphology of LCO particles. As can be seen, the agglomeration of RLCO750 particles decreases and

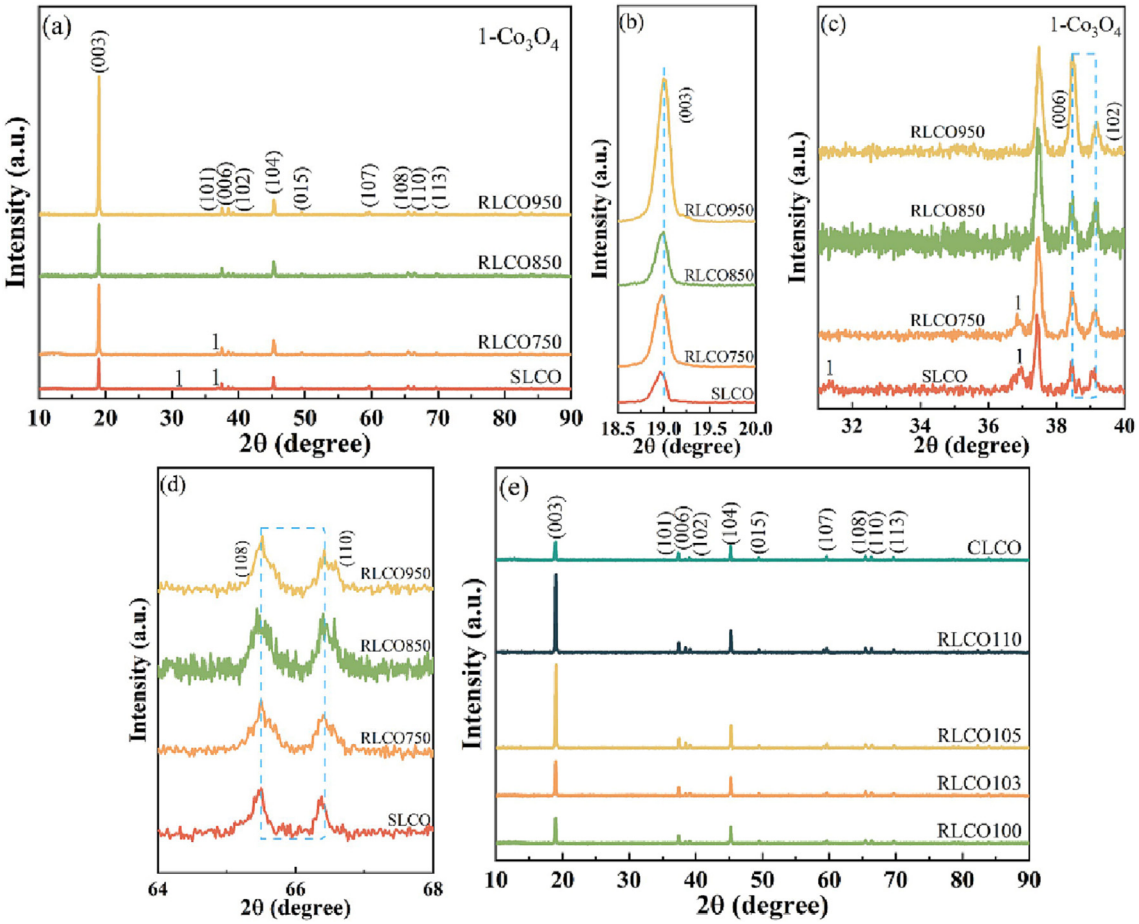

Fig. 2. XRD patterns of spend and regenerated samples under different temperatures at various 2θ range (a-d). XRD patterns of commercial LCO material and regenerated samples under different ratios of n(Li)/n(Co) (e).

the cracks on particles disappear. The layered structure could be detected, but surfaces of the particles are still rough. The regeneration reaction is incomplete at 750 °C, which is consistent with the XRD results. The RLCO850 and RLCO950 particles obtained at 850 and 950 °C have smoother surfaces and obvious layered structures. As can be realised, the RLCO950 particles are fragmented at high temperatures destroying the layered structure, which damages the electrochemical performance. By the increase of the n(Li)/n (Co) ratio, some flake-like small particles could be observed on the surface of the regenerated LCO particles, which may be the excess Li_2CO_3 covering the surfaces of the LCO particles.

The structure and the surface chemical composition of spent LCO and regenerated LCO materials were investigated by TEM and XPS, respectively. As shown in Fig. 4 (a), the surface structure of SLCO is seriously degraded, and it is difficult to observe clear lattice fringes. However, the regenerated RLCO100 material shows clear crystalline domains, which indicates the recovery of SLCO structure (Fig. 4 (b)). The wide-scan XPS spectra revealed a similar element composition of SLCO and RLCO100. However, the stronger Li 1s peak intensity of RLCO100 indicates that Li is re-embedded into the structure of SLCO material during the regeneration process (Fig. 4 (c) and (d)). The Co 2p XPS spectrum of SLCO and RLCO100 includes two shakeup satellite peaks and a double peak at the binding energies of 779.68 and 794.58 eV, assigned to Co $2p_{3/2}$ and Co $2p_{1/2}$, respectively. Two specific peaks (779.58 and 794.38 eV) corresponded to Co^{3+}, and the other two distinctive peaks (781.48 and 796.08 eV) corresponded to Co^{2+}. The content of Co^{3+} increased from 66.77% in spent LCO to 72.54% in the regenerated LCO, which reflects the effectiveness of structure regeneration, as shown in Fig. 4 (e) and (f).

3.2. Electrochemical characterisation and mechanism analysis

Fig. 5 shows the electrochemical performance of the spent and regenerated LCO materials treated at different temperatures. The initial discharge capacity of SLCO at 1C (1C = 150 mAg^{-1}) is only 21.7 mA h g^{-1}, and the discharge capacity after 100 cycles is further reduced to 1.4 mA h g^{-1}. The initial charge–discharge plateau of SLCO is very short, and its rate capability is significantly poor. From Fig. 5, it is evident that the electrochemical performance of SLCO is almost depleted. After regeneration, RLCO850 exhibits the best electrochemical performance due to its more complete layered structure, which is consistent with the XRD and SEM results. The initial discharge capacity of RLCO850 reaches 134.1 mA h g^{-1} under the current density of 1C (Fig. 5 (a)), while RLCO750 and RLCO950 exhibit capacities of 107.2 and 138.3 mA h g^{-1}, respectively. Besides, the discharge curves of regenerated materials all show a gentle voltage drop compared to SLCO, indicating low polarisation after regeneration (Fig. 5 (b)). RLCO850 also shows the highest rate performance. As shown in Fig. 5 (c), the RLCO850 produces the highest values of 151.8, 147.4, 141.7, 134.9, 125.9 and 104.2 mA h g^{-1} at 0.1C, 0.2C, 0.5C, 1C, 2C, 5C, respectively. After cycling at a high rate of 5C, the discharge capacity of RLCO850 could be recovered to 151.3 mA h g^{-1}, indicating that the repaired LCO structure is very stable.

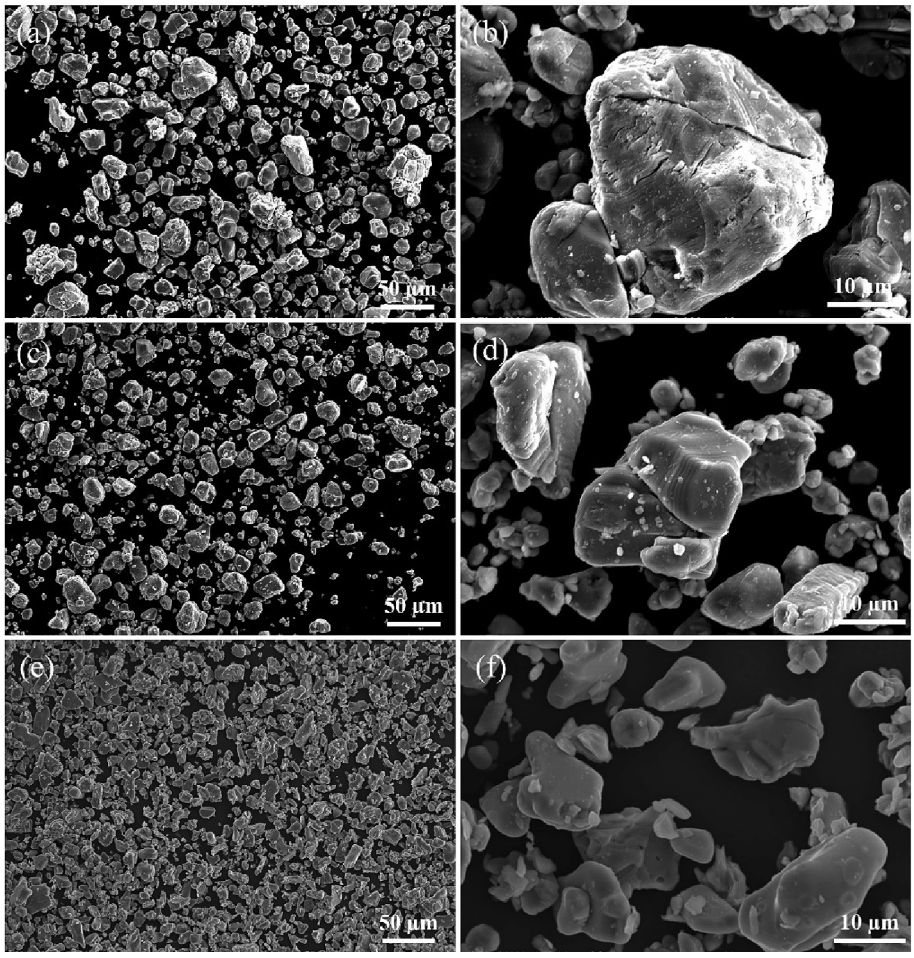

Fig. 3. SEM micrographs of SLCO: (a), (b), RLCO100: (c), (d) and CLCO: (e), (f).

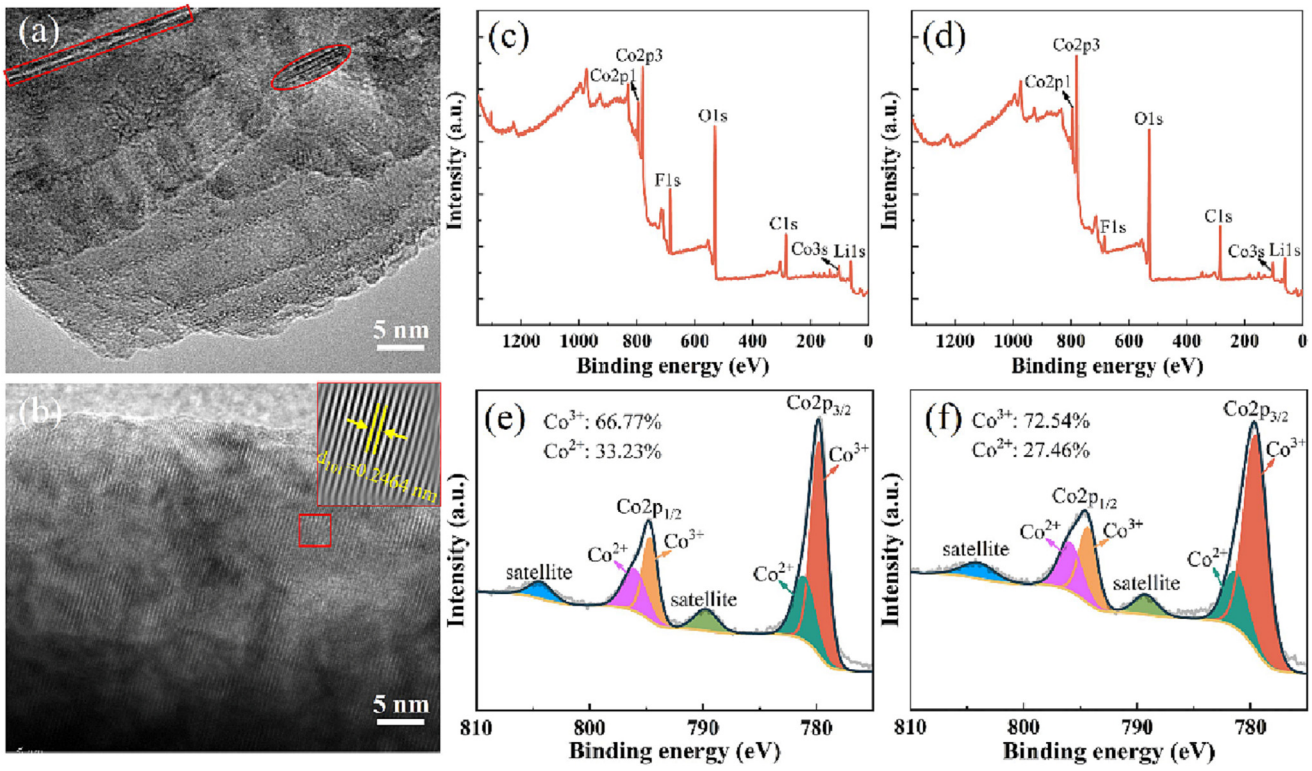

Fig. 4. TEM images, XPS survey spectra and high resolution spectra of Co 2p region recorded on SLCO: (a), (c), (e) and RLCO100: (b), (d), (f).

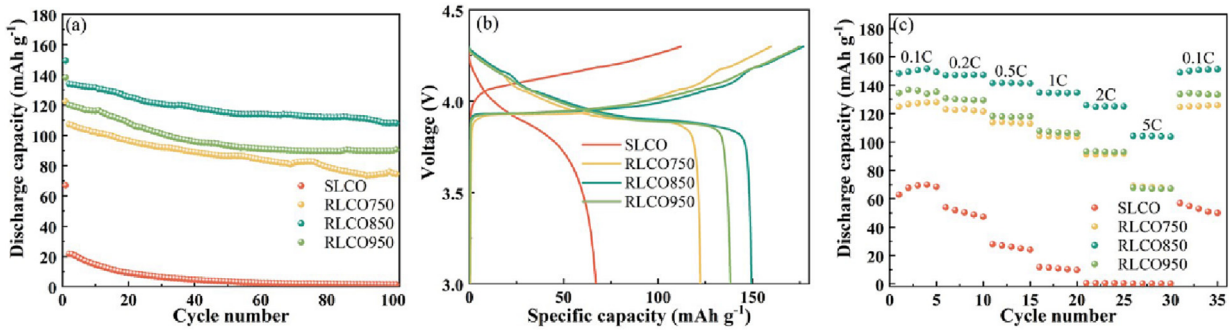

Fig. 5. Electrochemical performers of spent and regenerated LCO materials produced at different temperatures recorded at 3.0–4.3 V: (a) cycling performance at 1C, (b) charge–discharge curves, and (c) rate performance.

The electrochemical performance of commercial and regenerated LCO materials under different n(Li)/n(Co) ratios are displayed in Fig. 6. All regenerated samples show low polarisation, reaching the level of CLCO (Fig. 6 (a)). The RLCO100 sample is comparable with the other regenerated materials, exhibiting the highest initial discharge capacity of 138.9 mA h g^{-1} at 1C, while a capacity of 124.9 mA h g^{-1} is still maintained after 100 cycles corresponding to 89.9% capacity retention. In contrast, the fresh CLCO could only maintain 79.5% of its initial capacity after 100 cycles. In addition, the phase of RLCO100 and CLCO materials after a long cycle remains LCO, and no impurity phase is generated, which indicates the stability of the structure of the regenerated materials, as shown in Fig. S5. The regenerated samples all exhibit good rate performance, even better than the discharge capacity of CLCO at high current densities. The discharge capacity of RLCO100 at 2C and 5C is 128.4 and 111.3 mA h g^{-1}, while the discharge capacity of CLCO is 129.9 and 101.8 mA h g^{-1}. Based on this, the cycling performance of regenerated samples and CLCO were tested at 5C, as shown in Fig. 6 (d). Compared with CLCO, RLCO100 and RLCO103 exhibit better cycling stability at high current density. After 300 cycles, the capacity retention rates of CLCO, RLCO100 and RLCO103 are 53.5%, 62.9% and 49.8%, respectively. RLCO100 material shows an excellent discharge capacity, cycle stability and rate performance, which is particularly obvious at high current densities.

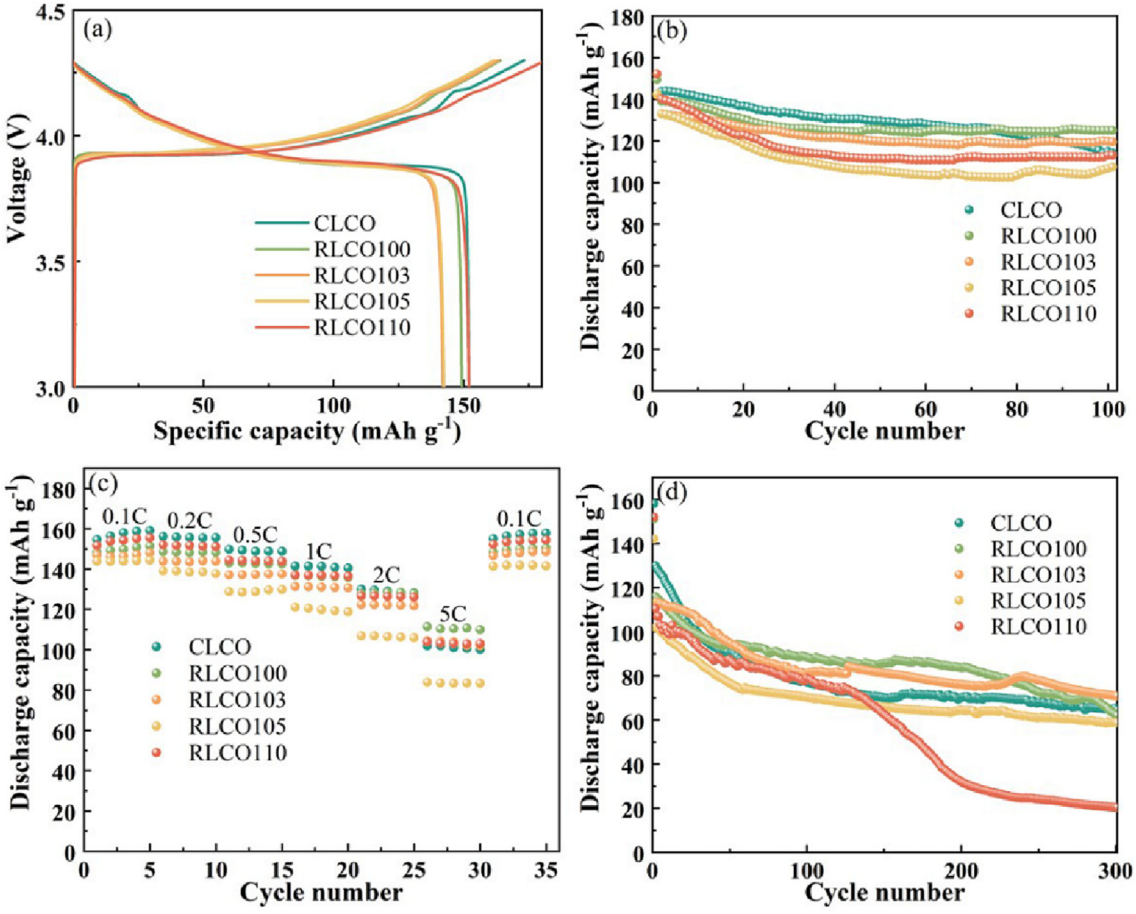

Fig. 6. Electrochemical performers of commercial and regenerated LCO materials produced under different n(Li)/n(Co) ratios recorded at 3.0–4.3 V: (a) charge–discharge curves, (b) cycling performance at 1C, (c) rate performance and (d) cycling performance at 5C.

Based on the above results, the optimal conditions for the solid-state synthesis regeneration process are the regeneration temperature of 850 °C and n(Li)/n(Co) ratio of 1:1. The solid-state synthesis method is shown to be effective for direct repair of completely failed LCO. Moreover, the electrochemical properties of the regenerated materials obtained from the three parallel experiments under the optimal regeneration conditions show little difference, which verifies the excellent reproducibility of the solid-state synthesis method to directly repair the completely failed cathode materials (Fig. S6).

The superior electrochemical performance of the regenerated samples over the fresh CLCO is particularly interesting. To understand the route of the enhanced performance, we conducted several CV and EIS analyses on all samples. The CV and Nyquist plots of different samples are shown in Fig. 7. The CV of SLCO material shows a significant polarisation phenomenon (Fig. 7 (a)), with almost none of the redox peaks typically observed for LCO. On the other hand, The CV curves of regenerated LCO have two reversible redox couples at 4.14/3.82 V and 4.21/4.08 V (Fig. 7 (b) and Fig. S7). Similar peaks, which correspond to the two-step oxidation/reduction of Co^{3+}/Co^{4+}, can also be detected at almost the same potential for the CLCO (Fig. 7 (c)). During the second and third cycles, the CV curves have almost highly overlapped redox peaks, which demonstrate the good reversibility of regenerated LCO. The semicircle corresponding to SLCO exhibits a larger diameter in EIS results (Fig. 7 (d)), indicating the higher charge-transfer impedance (R_{ct}, the value is same as R_2) at the interface between the SLCO electrode and electrolyte, as shown in Table S3. As mentioned before, this is attributed to the lack of Li^+ in SLCO, resulting in the change of layered structure and the formation of spinel phase Co_3O_4 with low Li ion conductivity. Increasing the level of the cracks also contributes to the low ionic conductivity of SLCO. The increased effective surface of SLCO induced by the structural defects is also responsible for high Warburg resistance at a low frequency. The R_{ct} value of regenerated LCO is smaller than SLCO and even smaller than that of CLCO (Table S3). The larger lattice parameters of the reconstructed layered structure are beneficial to promote more Li^+ transmission, indicating better electronic conductivity and kinetic performance (Table S2). Therefore, the electrochemical performance of the spent LCO material could be recovered to become even higher than commercial LCO.

3.3. Environmental and economic assessment

The EverBatt model developed by Argonne National Laboratory was employed to compare the economic and environmental impacts of direct regeneration, pyrometallurgical and hydrometallurgical recycling process in terms of cost and revenue, profit, energy consumption and greenhouse gas (GHG) emission (Fig. 8 (a)–(d)). The detailed process of using the EverBatt model evaluation can be found in Supplementary material. As shown in Fig. 8 (a) and (b), the battery fee accounts for the highest proportion of the recycling cost. The hydrometallurgical recycling process operates at low temperatures and does not require expensive equipment, resulting in the lowest recycling cost. The market prices of Li_2CO_3 are essential factors influencing the costs of the direct

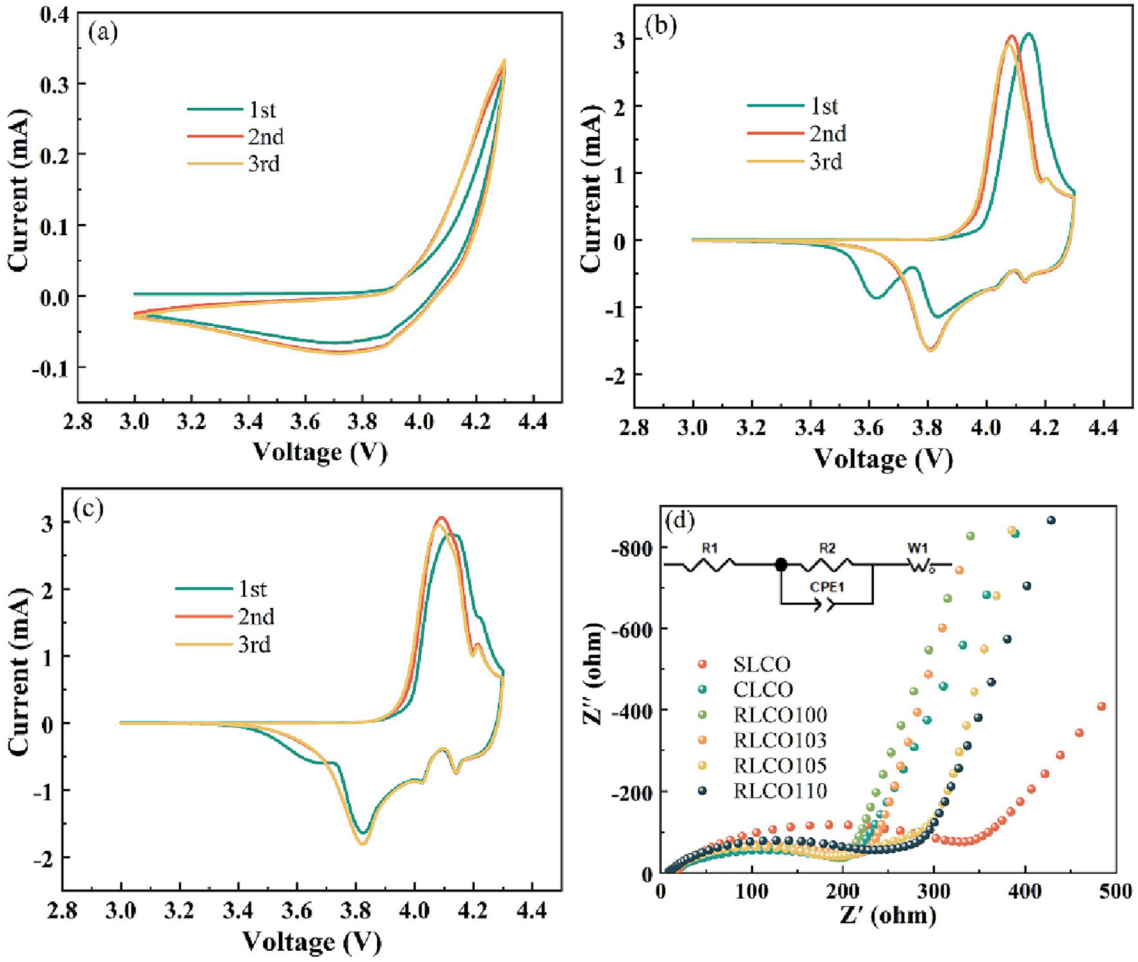

Fig. 7. CV curves of the first three cycles for (a) SLCO, (b) RLCO100 and (c) CLCO at a sweep rate of 0.2 mV s^{-1}. (d) Electrochemical impedance spectra (EIS) of different samples measured from 0.1 MHz to 0.01 Hz before cycling.

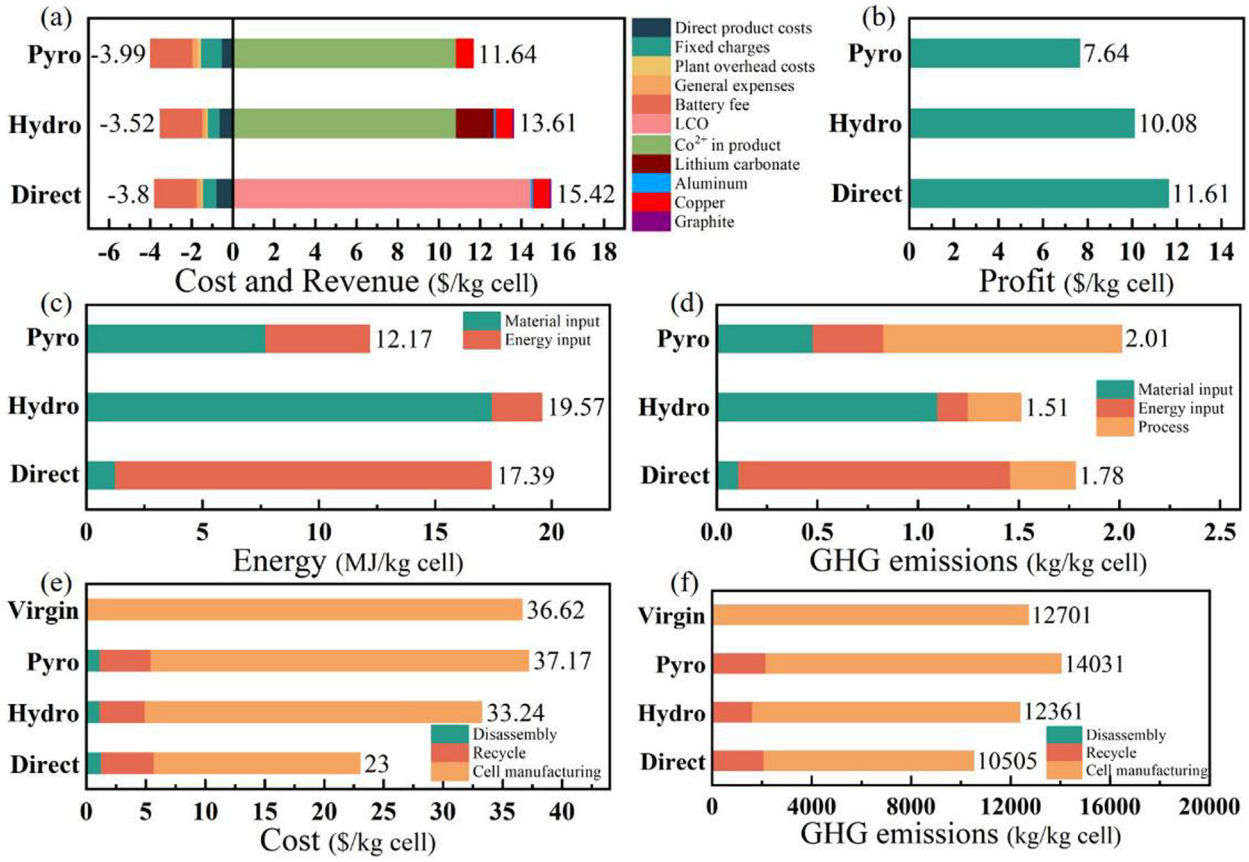

Fig. 8. Economic and environmental assessment of pyrometallurgical (Pyro), hydrometallurgical (Hydro) and direct regeneration methods (recycling 1 kg spent LCO batteries): cost and revenue (a), profit (b), energy consumption (c), GHG emissions (d). Comparison of different recycling methods and raw materials to produce 1 kg LCO batteries: total cost (e) and total GHG emissions (f).

regeneration process. In addition, direct regeneration has the highest revenue because the recycled cathode material can be directly used in producing LIBs, which is more valuable than the precursors produced by the pyrometallurgy and hydrometallurgy recycling processes. Therefore, direct regeneration has the highest profit ($ 11.61 per kilogram of recycled spent LCO batteries), while pyrometallurgy and hydrometallurgy are $ 7.64 and $ 10.08, respectively. The energy consumption of the pyrometallurgical, hydrometallurgical and direct regeneration recycling processes are 12.17, 19.57, and 17.39 MJ per kilogram of recycled spent LCO batteries, respectively (Fig. 8 (c)). The energy consumption of the pyrometallurgical and hydrometallurgical process mainly comes from the upstream production of input chemicals (The pyrometallurgical recycle process includes the subsequent alloy leaching and precipitation process). The GHG emissions of pyrometallurgy are mainly from the process emission (smelting), but the upstream manufacturing of chemicals contributes much to the GHG emissions from hydrometallurgy (Fig. 8 (d)). The energy consumption and GHG emissions of the direct regeneration process mainly come from fuel combustion and electricity due to the small input of raw materials and simple operation. Furthermore, the mild in-situ direct repair can provide an effective strategy for the future development of efficient technologies for the recycling of spent lithium-ion batteries reducing the associated environmental concerns.

In order to more accurately evaluate the three recycling methods and assess the potential of spent LIBs recycling, the environmental and economic assessment should focus on the entire closed-loop recycling process (disassembly, recycling and battery manufacturing), and compare it with the battery production process of raw materials (virgin), as shown in Fig. 8 (e) and (f). The total cost and total GHG emissions of the closed-loop recycling process mainly come from the battery manufacturing process. Compared with pyrometallurgy and hydrometallurgy, direct regeneration method has the smallest total cost and GHG emissions, which are $ 23 and 10505 kg per kilogram of produced LCO batteries, respectively. It is significantly lower than the raw material battery production process (cost: $ 36.62, GHG emissions: 12701 kg). It is much more economical to produce cathode materials directly from spent LIBs than raw materials. It avoids the use of expensive precursors and saves the conversion process of precursors, which greatly reduces the total cost and GHG emissions. Therefore, the direct regeneration method has significant economic benefits and environmental advantages.

4. Conclusions

The short-range and efficient Li replenishment regeneration of completely failed LCO cathode materials was realised by solid-state synthesis. The excessive loss of Li causes the change of layered structure and the generation of impurity Co_3O_4 phase, which leads to the complete failure of the electrochemical performance of spent LCO. The regenerated LCO materials showed significantly improved electrochemical performance (even better than the CLCO) under the optimal condition of 850 °C and n(Li)/n(Co) ratio of 1:1, consistent with its smooth surface and restored layered structure. Techno-economic analysis of the closed-loop recycling process shows that the direct regeneration method is a potentially green technology. Furthermore, the recycling of spent LIBs also involves the collection and transportation of batteries and the efficient crushing and clas-

sification of different components, all of which are necessary to achieve practical and profitable battery recycling.

CRediT authorship contribution statement

Lingyu Kong: Conceptualization, Methodology, Investigation, Formal analysis, Visualization, Writing – original draft. **Zhuo Li:** Conceptualization, Methodology, Investigation. **Wenhui Zhu:** Conceptualization, Methodology. **Chirag R. Ratwani:** Investigation, Visualization. **Niranjala Fernando:** Investigation, Visualization. **Shadeepa Karunarathne:** Investigation, Visualization. **Amr.M. Abdelkader:** Resources, Supervision, Funding acquisition, Conceptualization, Writing – review & editing. **Ali Reza Kamali:** Resources, Supervision, Funding acquisition, Conceptualization, Writing – review & editing. **Zhongning Shi:** Resources, Supervision, Conceptualization, Writing – review & editing.

Data availability

Data will be made available on request.

Declaration of Competing Interest

The authors declare that they have no known competing financial interests or personal relationships that could have appeared to influence the work reported in this paper.

Acknowledgments

Lingyu Kong holds a scholarship provided by the China Scholarship Council during the study at Bournemouth University. A.R. Kamali acknowledges the support from the National Natural Science Foundation of China (52250610222).

Appendix A. Supplementary material

Supplementary data to this article can be found online at https://doi.org/10.1016/j.jcis.2023.03.021.

References

[1] X.P. Chen, Y.B. Chen, T. Zhou, D.P. Liu, H. Hu, S.Y. Fan, Hydrometallurgical recovery of metal values from sulfuric acid leaching liquor of spent lithium-ion batteries, Waste Manage. 38 (2015) 349–356.
[2] S.A. Goncalves, E.M. Garcia, H.A. Taroco, R.G. Teixeira, K.J. Guedes, H.F. Gorgulho, P.B. Martelli, A.P.L. Fernandes, Development of non-enzymatic glucose sensor using recycled cobalt from cell phone Li-ion batteries, Waste Manage. 46 (2015) 497–502.
[3] L. Sun, K.Q. Qiu, Organic oxalate as leachant and precipitant for the recovery of valuable metals from spent lithium-ion batteries, Waste Manage. 32 (2012) 1575–1582.
[4] Y. Choi, S.W. Rhee, Current status and perspectives on recycling of end-of-life battery of electric vehicle in Republic of Korea, Waste Manage. 106 (2020) 261–270.
[5] X.L. Zeng, J.H. Li, L.L. Liu, Solving spent lithium-ion battery problems in China: opportunities and challenges, Renew. Sust. Energy Rev. 52 (2015) 1759–1767.
[6] S. Maroufi, M. Assefi, R.K. Nekouei, V. Sahajwalla, Recovery of lithium and cobalt from waste lithium-ion batteries through a selective isolation-suspension approach, Sust. Mater. Technol. 23 (2020) e00139.
[7] X.P. Chen, D.Z. Kang, L. Cao, J.Z. Li, T. Zhou, H.R. Ma, Separation and recovery of valuable metals from spent lithium ion batteries: simultaneous recovery of Li and Co in a single step, S Sep. Purif. Technol. 210 (2019) 690–697.
[8] J.F. Xiao, J. Li, Z.M. Xu, Challenges to future development of spent lithium ion batteries recovery from environmental and technological perspectives, Environ. Sci. Technol. 54 (2020) 9–25.
[9] P. Meister, H.P. Jia, J. Li, R. Kloepsch, M. Winter, T. Placke, Best practice: performance and cost evaluation of lithium ion battery active materials with special emphasis on energy efficiency, Chem. Mater. 28 (2016) 7203–7217.
[10] Y.C. Zhang, W.Q. Wang, Q. Fang, S.M. Xu, Improved recovery of valuable metals from spent lithium-ion batteries by efficient reduction roasting and facile acid leaching, Waste Manage. 102 (2020) 847–855.
[11] X.P. Chen, D.Z. Kang, J.Z. Li, T. Zhou, H.R. Ma, Gradient and facile extraction of valuable metals from spent lithium ion batteries for new cathode materials re-fabrication, J. Hazard. Mater. 389 (2020) 121887.
[12] Y. Shi, G. Chen, Z. Chen, Effective regeneration of $LiCoO_2$ from spent lithium-ion batteries: a direct approach towards high-performance active particles, Green Chem. 20 (2018) 851–862.
[13] X.H. Zheng, W.F. Gao, X.H. Zhang, M.M. He, X. Lin, H.B. Cao, Y. Zhang, Z. Sun, Spent lithium-ion battery recycling-reductive ammonia leaching of metals from cathode scrap by sodium sulphite, Waste Manage. 60 (2017) 680–688.
[14] J.F. Xiao, J. Li, Z.M. Xu, Recycling metals from lithium ion battery by mechanical separation and vacuum metallurgy, J. Hazard. Mater. 338 (2017) 124–131.
[15] R. Golmohammadzadeh, F. Rashchi, E. Vahidi, Recovery of lithium and cobalt from spent lithium-ion batteries using organic acids: process optimization and kinetic aspects, Waste Manage. 64 (2017) 244–254.
[16] M.M. Wang, C.C. Zhang, F.S. Zhang, Recycling of spent lithium-ion battery with polyvinyl chloride by mechanochemical process, Waste Manage. 67 (2017) 232–239.
[17] S. Natarajan, V. Aravindan, Burgeoning prospects of spent lithium-ion batteries in multifarious applications, Adv. Energy Mater. 8 (2018) 1802303.
[18] E. Fan, P. Shi, X.X. Zhang, J. Lin, F. Wu, L. Li, R.J. Chen, Glucose oxidase-based biocatalytic acid-leaching process for recovering valuable metals from spent lithium-ion batteries, Waste Manage. 114 (2020) 166–173.
[19] E. Fan, J.B. Yang, Y.X. Huang, J. Lin, F. Arshad, F. Wu, L. Li, R.J. Chen, Leaching mechanisms of recycling valuable metals from spent lithium-ion batteries by a malonic acid-based leaching system, ACS Appl. Energy Mater. 3 (2020) 8532–8542.
[20] L. Li, J.B. Dunn, X.X. Zhang, L. Gaines, R.J. Chen, F. Wu, K. Amine, Recovery of metals from spent lithium-ion batteries with organic acids as leaching reagents and environmental assessment, J. Power Sources 233 (2013) 180–189.
[21] D.A. Ferreira, L.M.Z. Prados, D. Majuste, M.B. Mansur, Hydrometallurgical separation of aluminium, cobalt, copper and lithium from spent Li-ion batteries, J. Power Sources 187 (2009) 238–246.
[22] Y.L. Zhao, X.Z. Yuan, L.B. Jiang, J. Wen, H. Wang, R.P. Guan, J.J. Zhang, G.M. Zeng, Regeneration and reutilization of cathode materials from spent lithium-ion batteries, Chem. Eng. J. 383 (2020) 123089.
[23] Y.F. Huang, G.H. Han, J.T. Liu, W.C. Chai, W.J. Wang, S.Z. Yang, S.P. Su, A stepwise recovery of metals from hybrid cathodes of spent Li-ion batteries with leaching-flotation-precipitation process, J. Power Sources 325 (2016) 555–564.
[24] E. Fan, L. Li, Z.P. Wang, J. Lin, Y.X. Huang, Y. Yao, R.J. Chen, F. Wu, Sustainable recycling technology for Li-ion batteries and beyond: challenges and future prospects, Chem. Rev. 120 (2020) 7020–7063.
[25] G. Harper, R. Sommerville, E. Kendrick, L. Driscoll, P. Slater, R. Stolkin, A. Walton, P. Christensen, O. Heidrich, S. Lambert, A. Abbott, K. Ryder, L. Gaines, P. Anderson, Recycling lithium-ion batteries from electric vehicles, Nature 575 (2019) 75–86.
[26] Y. Shi, G. Chen, F. Liu, X.J. Yue, Z. Chen, Resolving the compositional and structural defects of degraded $LiNi_xCo_yMn_zO_2$ particles to directly regenerate high-performance lithium-ion battery cathodes, ACS Energy Lett. 3 (2018) 1683–1692.
[27] M.J. Ganter, B.J. Landi, C.W. Babbitt, A. Anctil, G. Gaustad, Cathode refunctionalization as a lithium ion battery recycling alternative, J. Power Sources 256 (2014) 274–280.
[28] X.L. Li, J. Zhang, D.W. Song, J.S. Song, L.Q. Zhang, Direct regeneration of recycled cathode material mixture from scrapped $LiFePO_4$ batteries, J. Power Sources 345 (2017) 78–84.
[29] A.R. Kamali, J. Ye, Reactive molten salt modification of ilmenite as a green approach for the preparation of inexpensive Li ion battery anode materials, Miner. Eng. 172 (2021) 107175.
[30] J. Yang, W.Y. Wang, H.M. Yang, D.H. Wang, One-pot compositional and structural regeneration of degraded $LiCoO_2$ for directly reusing it as a high-performance lithium-ion battery cathode, Green Chem. 22 (2020) 6489–6496.
[31] R.P. Li, A.R. Kamali, Molten salt assisted conversion of corn lignocellulosic waste into carbon nanostructures with enhanced Li-ion storage performance, Chem. Eng. Sci. 265 (2023) 118222.
[32] Q.K. Jing, J.L. Zhang, Y.B. Liu, W.J. Zhang, Y.Q. Chen, C.Y. Wang, Direct regeneration of spent $LiFePO_4$ cathode material by a green and efficient one-step hydrothermal method, ACS Sust. Chem. Eng. 8 (2020) 17622–17628.
[33] L.G. Zhang, Z.M. Xu, Z. He, Electrochemical relithiation for direct regeneration of $LiCoO_2$ materials from spent lithium-ion battery electrodes, ACS Sust. Chem. Eng. 8 (2020) 11596–11605.
[34] J.W. Wu, J. Lin, E. Fan, R.J. Chen, F. Wu, L. Li, Sustainable regeneration of high-performance $Li_{1-x}Na_xCoO_2$ from cathode materials in spent lithium-ion batteries, ACS Appl. Energy Mater. 4 (2021) 2607–2615.
[35] Y. Gao, Y. Li, J. Li, H.Q. Xie, Y.P. Chen, Direct recovery of $LiCoO_2$ from the recycled lithium-ion batteries via structure restoration, J. Alloys Compd. 845 (2020) 156234.
[36] E. Fan, J. Lin, X.D. Zhang, R.J. Chen, F. Wu, L. Li, Resolving the structural defects of spent $Li_{1-x}CoO_2$ particles to directly reconstruct high voltage performance cathode for lithium-ion batteries, Small Methods 5 (2021) 2100672.
[37] Z.X. Chi, J. Li, L.H. Wang, T.F. Li, Y. Wang, Y.Y. Zhang, S.D. Tao, M.C. Zhang, Y.H. Xiao, Y.Z. Chen, Direct regeneration method of spent $LiNi_{1/3}Co_{1/3}Mn_{1/3}O_2$ cathode materials via surface lithium residues, Green Chem. 23 (2021) 9099–9108.